Micromeritical Properties of Snow*

Daisuke KUROIWA
黒 岩 大 助
The Institute of Low Temperature Science, Hokkaido University, Sapporo, Japan
Yukiko MIZUNO
水 野 悠 紀 子
Department of Physics, Hokkaido University of Education, Sapporo, Japan
and
Masao TAKEUCHI
竹 内 政 夫
Civil Engineering Research Institute, Hokkaido Development Bureau, Sapporo, Japan

Abstract

Snow particles easily adhere and join together, and form a consistent snow aggregate, the so-called "snow cover" or "deposited snow". Aggregation of snow depends to a considerable extent upon its surface roughness and mutual cohesion. To date, many research papers on physical properties of snow cover have been published, but little work has been done to study snow particles from a point of the micromeritics. In this paper, a simple definition of the surface roughness is given for natural snow crystals and pulverized snow particles, and their micromeritical properties such as angle of repose, internal friction, packing by tapping, age hardening and capillary potential are analyzed and discussed with reference to the sintering or consolidation process.

Introduction

Snow crystals gradually change their shapes without being subjected to thawing and turn into fine spherical ice particles after they have precipitated on the ground. These ice particles join together and form a "deposited snow" or "snow cover". When snow crystals come down from the sky, they are interlocked each other and form a consistent aggregate. The consistency of these aggregates depends largely on the surface irregularities and proper cohesion between crystals or particles. The proper cohesion occurs by molecular cohesion which depends upon temperature. When two ice particles or snow crystals are brought into contact, an ice bond is rapidly formed at the contact point by the transportation of the water molecules. Both the surface irregularities and proper cohesion may play important roles on the micromeritical properties of snow. A natural snow cover or densified snow can be regarded as a kind of porous ceramic which consists of ice particles, because ice particles are readily sintered and consolidated at ordinary climatical low temperatures. Physical properties of snow, as a porous solid body, have been studied by many authors, but few studies have been made from the point of the micromeritics or physics of powder. The present paper deals with snow and snow crystals as powdered materials. The paper consists of four sections:

* Contribution No. 788 from The Institute of Low Temperature Science, Hokkaido University.

Section I. Surface Irregularities of Snow Crystals and Pulverized Snow
Section II. Angle of Repose of Snow
Section III. Compaction of Snow by Tapping
Section IV. Age Hardening and Capillary Potential of Snow Aggregates

When snow crystals or ice particles are treated as powder, complex problems may arise from their surface irregularities and mutual adhesion. In the first section, a simple definition on surface roughness or irregularities of snow crystals and ice particles will be given as one of the most basic properties of powder. The second and third sections will deal with the problem of the angle of repose and the compaction by tapping of snow in which the surface properties of particles may play important roles. As has been noted by many authors, ice or snow particles easily adhere and join together and turn into a solid mass. Therefore, most of the physical properties of a snow aggregate vary as a function of time and temperature. In the final section, the age hardening and capillary potentials of snow aggregates will be discussed from the point of sintering.

I. Surface Irregularities of Snow Crystals and Ice Particles

When snow crystals come down from the sky, they are interlocked with each other and form snow aggregates or snow flakes. The probability of the occurrence of the interlocking may be primarily dependent upon the surface roughness of the crystals. Morphological classification of snow crystals has been made by Nakaya (1954), and they were classified into several types, needle, dendritic, plate, columnar, and so forth. Among these crystals, the dendritic may be considered to be the most probable crystal to form a snow aggregate in the air, because of its complex shape. The consistency of a snow aggregate depends not only upon the surface irregularities of the crystals, but also it depends on the ice bonding or proper cohesion between crystals. The strong ice bonds developed at the contact points keep aggregates from mechanically disintegrating. As a growth rate of the ice bond increases with the ambient air temperature, the probability to form snow aggregates may increase with air temperatures.

Since the precise definition of the surface irregularity of snow crystals was difficult, the following two definitions were used for the convenience sake in this paper. A typical dendritic snow crystal and two circles are shown in Fig. 1. We shall denote a projected area and a total length of the periphery of this dendritic crystal as A and P. The projected area and periphery were measured by a planimeter and kilbimeter. Two circles A and B were depicted in such a way that the circle A has the same area with the projected area of the crystal and the circle B has the same length of the periphery with that of the crystal. Therefore, the length of the periphery of the circle A is smaller than that of the original crystal, while the area of the circle B is larger than that of the crystal. If we take the following two ratios:

$\varepsilon_a = \frac{P}{p}$ ratio of the total length of the periphery of the crystal against the length of the periphery of the circle A (definition by periphery),

$\varepsilon_b = \frac{B}{A}$ ratio of the area of the circle B against the projected area of the crystal A (definition by area),

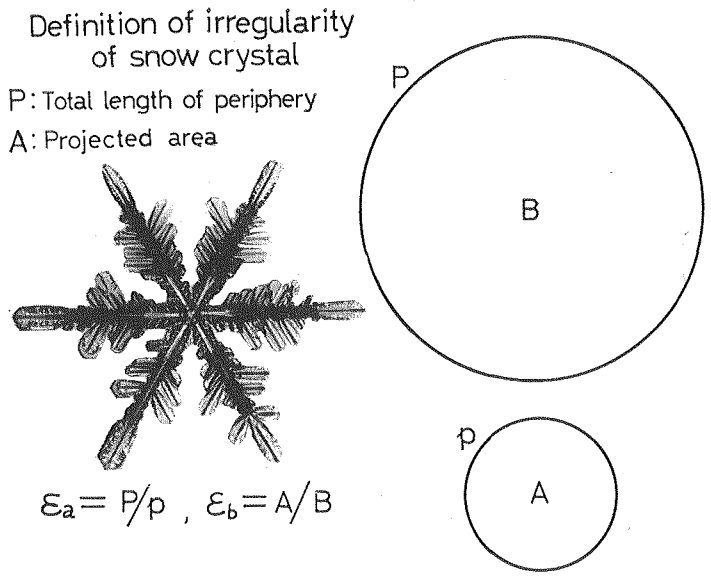

Fig. 1. Definition of irregularity of snow crystal

the irregularity of snow crystal can be defined by either the ratio ε_a or ε_b. According to the definitions, there may be the following correlation between these two ratios:

$$\varepsilon_a = \varepsilon_b^2 .$$

Microphotographs of various types of snow crystals are shown in Fig. 2. a, b and c are dendritic, d the needle, e the columnar, and f the plate-like crystals. The observed numerical values of ε_a and ε_b are given for each crystal. As seen in these pictures, the dendritic crystals have larger values of the irregularities than those of the needle and columnar crystals.

In order to measure surface irregularities of the pulverized snow particles, two blocks of snow were rubbed against each other and ground into fine powder. Figure 3 shows microphotographs of the typical particles of this pulverized snow. The observed values of both ε_a and ε_b are given for each particles. As seen in these pictures, values of the irregularities of the pulverized snow particles are very small and near unity, because their shapes are rounded and spherical. However, the projected area of pulverized snow particles may vary with the angle of vision, implying that the numerical values of the irregularities of spherical ice particles would not be uniquely determined. In order to demonstrate how the projected area of one spherical particle changes with the angle of vision, three microphotographs of the same ice particle were taken from different angles. These three pictures are shown in Fig. 4, but little differences may be found in the observed values of the irregularities as seen in this figure. Therefore, the difference of surface irregularities of the pulverized snow particle caused by different angles of vision can be considered to be small in the practical sence.

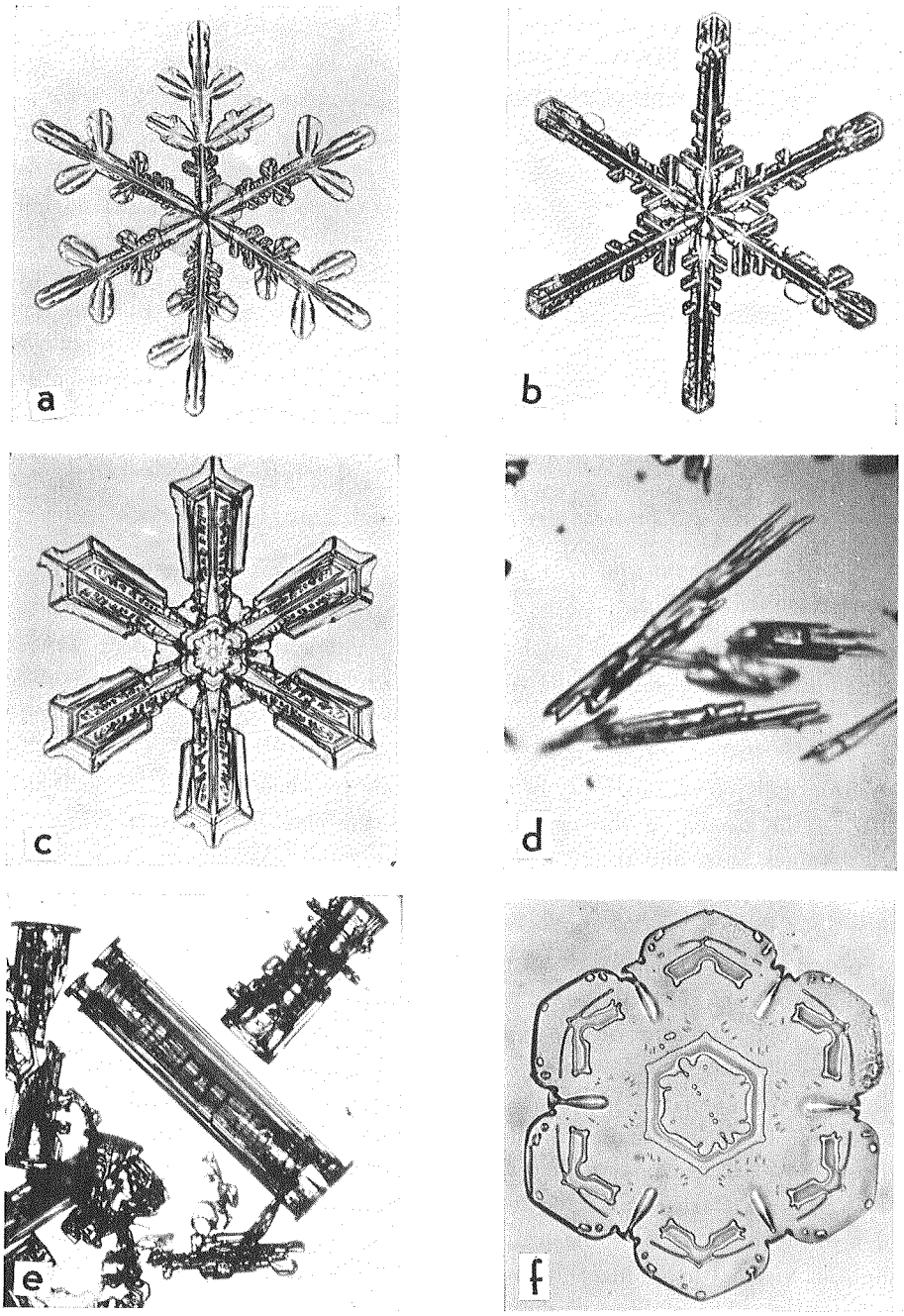

Fig. 2. Surface irregularities of various kinds of snow crystals

a : $\varepsilon_a = 42.5$, $\varepsilon_b = 6.5$
b : $\varepsilon_a = 21.3$, $\varepsilon_b = 4.61$
c : $\varepsilon_a = 6.8$, $\varepsilon_b = 2.61$
d : $\varepsilon_a = 5.52$, $\varepsilon_b = 2.35$
e : $\varepsilon_a = 2.6$, $\varepsilon_b = 1.61$
f : $\varepsilon_a = 1.47$, $\varepsilon_b = 1.21$

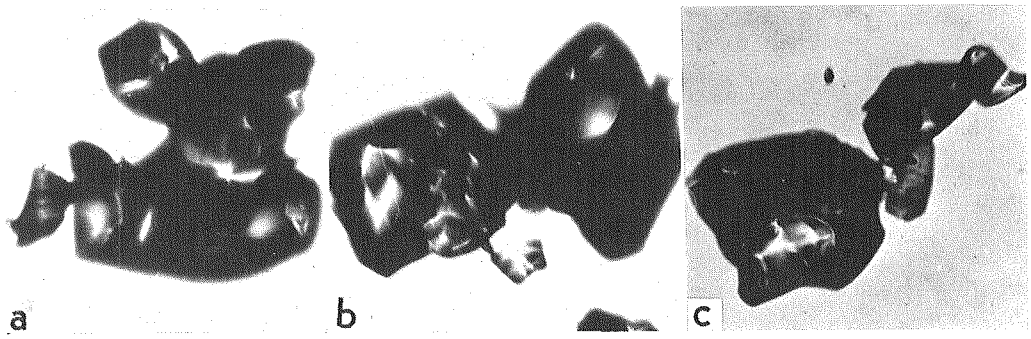

Fig. 3. Surface irregularities of pulverized snow particles
a : $\varepsilon_a = 2.08$, $\varepsilon_b = 1.44$ b : $\varepsilon_a = 1.75$, $\varepsilon_b = 1.32$ c : $\varepsilon_a = 2.86$, $\varepsilon_b = 1.69$

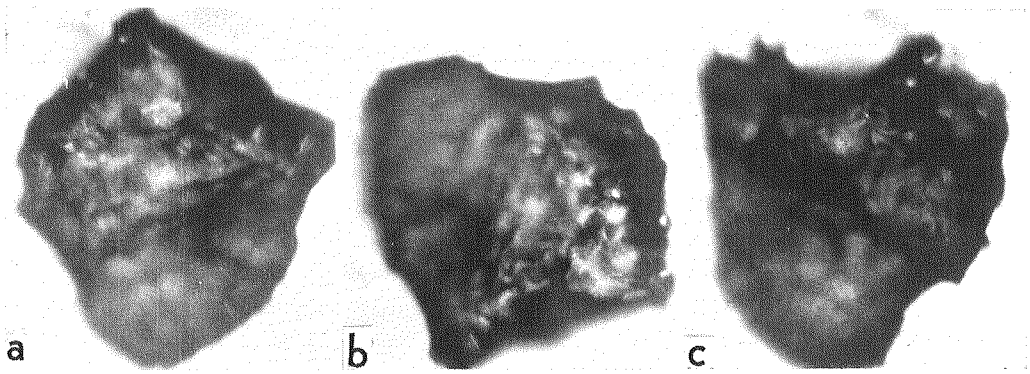

Fig. 4. Change of irregularity of one particle observed from different angle of vission
a : $\varepsilon_a = 1.1$, $\varepsilon_b = 1.05$ b : $\varepsilon_a = 1.2$, $\varepsilon_b = 1.1$ c : $\varepsilon_a = 1.28$, $\varepsilon_b = 1.12$

II. Angle of Repose of Snow

1) *Definition and how to measure the angle of repose of snow*

Angle of repose is refered to as one of the most important properties of micromeritics. If powdery pulverized solid particles are dropped gently through a nozzle of a hopper on the surface of the disk placed right underneath the nozzle, they begin to pile up on the disk in the form of a cone. The diameter and height of the cone increase with time. When the periphery of the cone reaches the edge of the disk, the height of the cone becomes constant, because the excess particles begin to slide down along the slope of the cone. In this steady state, the angle between the slope of the cone and the disk is called the "angle of repose". The angle of repose depends greatly upon surface irregularities and mutual adhesion of particles. If both irregularities and adhesion are large, the angle of repose becomes large, and the reverse may be true.

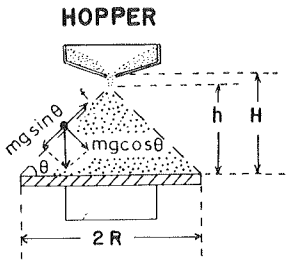

Fig. 5. Definition of angle of repose

As seen in Fig. 5, the following simple mechanical correlation may be applied for a particle lying on the

slope of the cone:

$$f = mg \cdot \sin\theta = \mu mg \cdot \cos\theta \,, \tag{1}$$

where f is the frictional force required to prevent the sliding of the particle down along the slope, and m is the mass of the particle, g the graviational acceleration, μ the coefficient of the internal friction between particles, θ the angle of repose. From this formula, it may be clear that μ is closely correlated to the angle of repose θ. We obtain

$$\mu = \tan\theta = h/R \,, \tag{2}$$

where h is the height of the cone, R the radius of the disk. Therefore, the angle of repose θ is given by

$$\theta = \tan^{-1}(h/R) \,. \tag{3}$$

A large hopper, with a mouth-diameter of 20 cm and a nozzle-diameter of 1 cm was mounted vertically on the table, and a disk was placed under the nozzle. Two blocks of snow were pulverized right above the hopper by rubbing two snow blocks together. The powdery pulverized snow particles were dropped through the nozzle and piled up on the disk. In the case of the natural snow crystals a small amount of crystals were continuously fed into the hopper. Sometimes, a slight shock was applied to the hopper to avoid blocking up of the nozzle with crystals. When the nozzle of the hopper became blocked with snow crystals or ice particles, they were forced out of the nozzle by a small glass stick.

In this experiment, a question may arise as to how to determine the drop height H (distance between the nozzle and the disk), and the radius R of the disk. If H is taken too large in comparison with the diameter of the disk used, the dropping particles do not pile up on the disk in the form of cone, because of the strong impaction of particles. On the contrary, if H is too short in comparison with the diameter of the disk, the top of the cone may reach the nozzle, and the result may be unfavorable. Figures 6 A and B show how the angle of repose was influenced by the drop height H. In this experimentation, a 10 cm disk was used, and H was taken as 25 cm for A and 10 cm for B. This picture proves that the top of snow cone is rounded by the strong

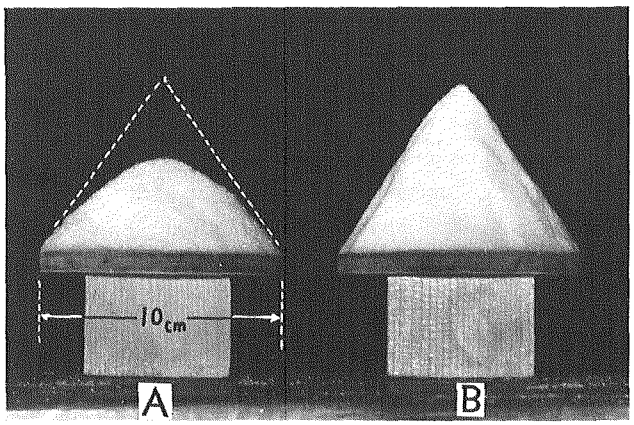

Fig. 6. Snow cones showing an effect of different drop height
A: $H = 25$ cm, B: $H = 10$ cm

mechanical impaction of ice particles when H was taken as 2.5 times larger than the diameter of the disk. Therefore, some rule should be set with respect to the method of measurment of the angle of repose. According to our experiments, when H was taken as a height lesser than the diameter of the disk, reasonable data were obtained for pulverized snow, but H had to be taken as 2 or 2.5 times larger than the diameter of the disk for natural snow crystals. In order to examine the influence of the size of the disk on the angle of repose, three kinds of disks, 16, 10 and 7 cm in diameters, were tested, but no difference was observed within experimental errors. Therefore, a 10 cm disk was used in our experiments. Accuracy of the measurement of the angle of repose was approximately $\pm 30'$.

2) *Angle of repose of pulverized snow particles*

Figure 7 shows the temperature dependence of the angle of repose of the pulverized snow. The average grain size of the particles was approximately 0.5~0.6 mm, and the observed surface irregularities ranged between $\varepsilon_a = 1 \sim 2.5$. The measurements were conducted at various temperatures in the range of $-35 \sim +1$°C, the drop height H was taken as 7 cm. The value of angle of repose observed at the temperatures -35 and -20°C was 45 deg as shown in A of Fig. 7. This means that the coefficient of the

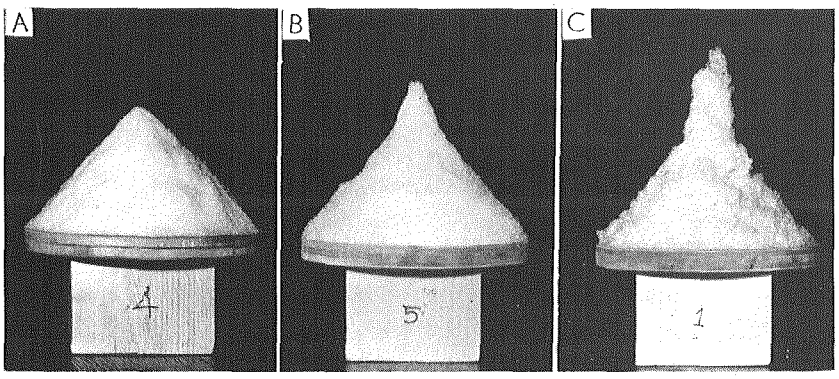

Fig. 7. Temperature dependence of angle of repose of pulverized snow
A: -35°C, B: -3.5°C, C: 0°C

internal friction between particles can be considered to be unity~1. However, the angle of repose increased with the temperature as 47 deg for -12°C and 50 deg and 11′ for -6°C. When the experiment was made at -3.5°C, the top of the snow cone began to grow sharply upwards as seen in B of Fig. 7. In this case, the value of angle of repose was estimated roughly as 55 deg. This temperature dependence implies that the cohesive force of ice begins to exert its influence on the angle of repose with the rise in temperature. In order to measure the angle of repose of wet snow particles, an experiment was made at room temperature $+1$°C. At this temperature, the surface of ice particles were covered with a thin water film and they clung to each other. The wet snow was forced out from the hopper nozzle. When the height of cone reached appoximately 5 cm, wet snow begun to accumulate chimney fashion at the top of the snow cone as seen in C of Fig. 7. This suggests that the liquid film acts as an intermediate agent to atract ice particles to each other, and that the angle of repose of wet snow can be considered to be

nearly 90 deg. The observed temperature dependence of the angle of repose is depicted by curve A in Fig. 8. In this figure, curve B represents another experimental result of the angle of repose measured with the drop height $H=10$ cm. A little difference can be seen in the two curves, but the angle of repose showed a tendency to approarch 90 deg with the increasing temperatures.

If the angle of repose depends only upon the surface irregularities of particles, the temperature dependence may not be observed, because the surface irregularity depends only upon the geometrical shape of the particle, but not on the temperature. The experimental results shown in Fig. 8 suggest that the proper cohesion of ice begins to

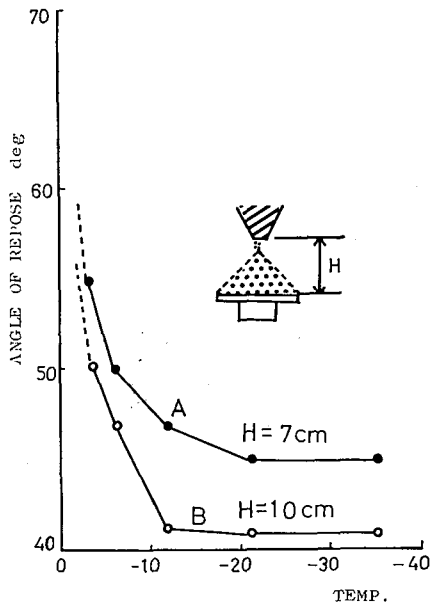

Fig. 8. Temperature dependence of angle of repose of pulverized snow

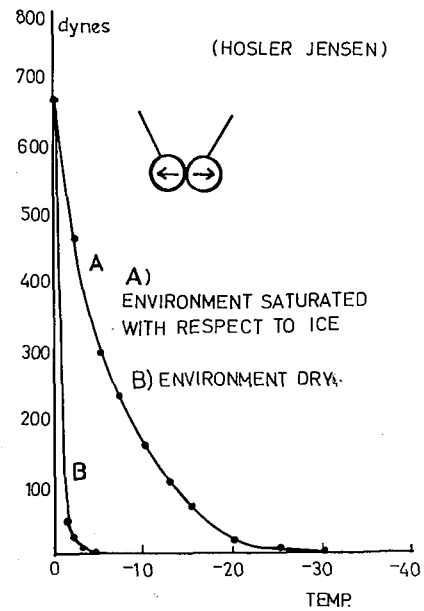

Fig. 9. Temperature dependence of cohesive force between two ice spheres (Hosler and Jensen, 1957)

act with the elevated temperatures. Figure 9 shows the temperature dependence of the force required to separate two ice spheres. This result was obtained by Hosler and Jensen (1957). In this experiment, the force was measured in both dry and wet environments with respect to ice, after two ice spheres had been brought into contact for one minute. As seen in this figure, the cohesive force increased with the increasing temperatures in the saturated enviroment A, but it was slight under the unsaturated enviroment B. In our experiment, almost all measurements were conducted in cold rooms almost saturated with respect to ice. Therefore, it may be reasonable to expect that the cohesive force began to exert its strong influence on the angle of repose when the air temperature approached the melting point of ice. Hosler and Jensen, and Nakaya and Matsumoto (1954) proposed the existence of a liquid like film on ice surface as the origin of the adhesion of ice. Kingery (1960) and Kuroiwa (1961) showed that ice sintering or ice bonding occurred between ice spheres when they were brought into contact with each other. Apart from the mechanism of the cohesion of ice, it may be

concluded that the angle of repose of the pulverized snow varies from 45 to 55 deg in the range of $-35\sim-3.5$°C, and it approaches 90 deg near the melting point.

3) *Particle size dependence of the angle of repose*

In order to examine the influence of the particle size of snow on the angle of repose, the pulverized snow particles were sieved into three classes A (5~2 mm), B (2~0.84 mm), and C (0.84~0.42 mm). Class A means that the ice particles passed 5mm openings of the sieve and were retained by 2 mm openings. Similary, the numbers enclosed with the brackets mean the range of particle size of the class. The average grain sizes of these three classes can be regarded as 3.5 mm for *A*, 1.42 mm for *B*, and 0.63 mm for *C*. The experiments were conducted in a cold room maintained at −35°C in order to exclude the influence of cohesive force on the angle of repose. The observed data are listed in the Table 1.

Table 1. Influence of particle size on the angle of repose

Class	Opening of sieve	Average grain size	Angle of repose at −35C°
A	5~2 mm	3.5 mm	40 deg
B	2~0.84 mm	1.42 mm	41 deg
C	0.84~0.42 mm	0.63 mm	42 deg

As seen in this table, the angle of repose increases slightly with the decreasing grain size, implying that relatively small ice grains may have larger surface irregularities than those of large grains.

4) *Angle of repose of natural snow crystals*

Most of the snow crystals found in the middle latitudes are composed of various types of dendrites as shown in a, b and c of Fig. 2. The observed values of irregularities of these crystals ranged between 40~10. These large numbers of irregularities may be responsible for the mechanical interlocking of snow crystals. Figure 10 shows the temperature dependence of the angle of repose of the dendritic snow crystals. In these experiments, the drop height H was taken as 25 cm. Picture A shows the snow

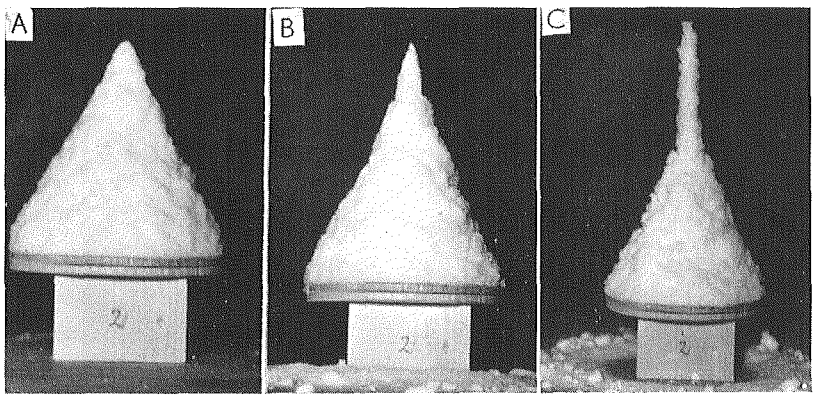

Fig. 10. Temperature dependence of angle of repose of dendritic snow crystals A: −35°C, B: −12°C, C: −4°C

cone piled up on the disk at −35°C. As seen in A, the angle of repose was found to be approximately 63 deg. This value was very large in comparison with that of the pulverized snow obtained at the same temperature. The large values of the surface irregularities of the natural snow crystals must be the main reason for high value of the angle of repose of the natural snow crystals, because the cohesive force was very faint at this low temperature. However, when the temperature was elevated to −12°C, the top of snow cone began to grow sharply as seen in B, implying that the cohesive force began to exert its influence on the angle of repose. Picture C of Fig. 10 shows the chimney like accumulation at the top of the snow cone obtained at −4°C. Therefore, the angle of repose of the dendritic snow crystals may be very close to 90 deg at high temperatures.

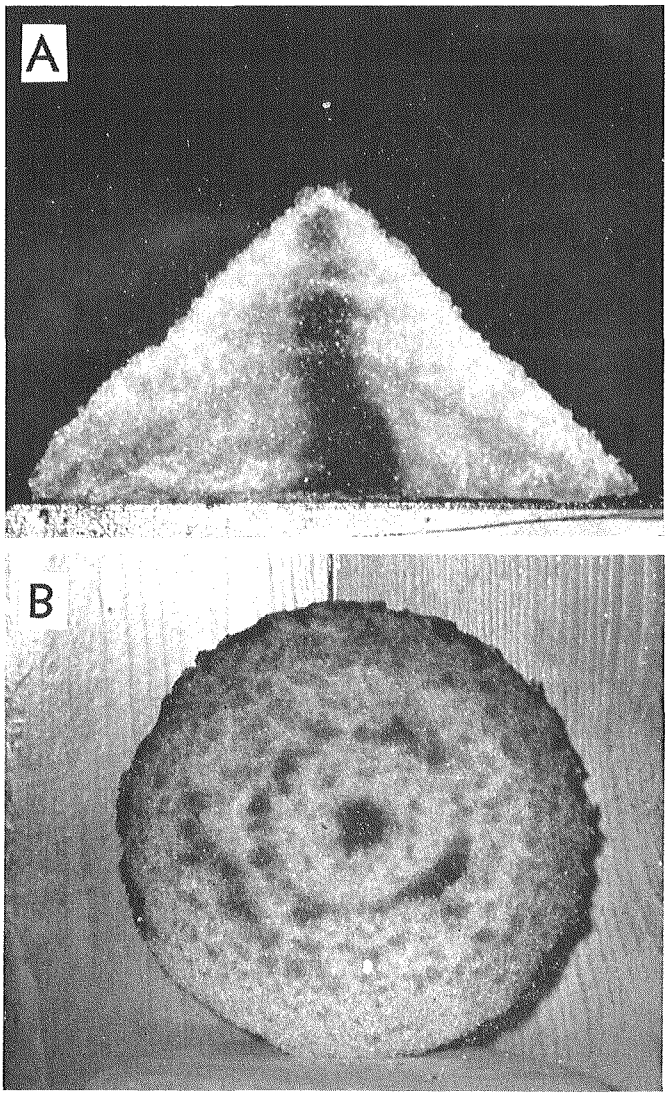

Fig. 11. Cross sections of snow cones. A: Vertical, B; Horizontal

5) *Internal structure of snow cone*

It may be interesting to show the internal structure of the snow cone. After the angle of respose was measured, snow cones were stored in the cold room for several days, and then they were cut vertically or horizontally into two parts. When a warm water colored with blue ink was sprayed on the surfaces of these cross sections, characteristic patterns appeared as seen in Fig. 11. A and B show the vartical and the horizontal sections. The thick bluish pattern indicates a densified structure which consists of fine grains, and the lightly bluish portion means a comparatively spacious structure composed of coarse grains, because fine grains can more readily sustain the blue ink than coarse grains. As seen in Fig. 11, a heavily colored zone existed at the center of the snow cone, implying that the fine particles were piled preferentially at the center of the cone.

III. Compaction of Snow by Tapping

1) *Compaction process by tapping*

When powdery pulverized solid particles are packed, it is very difficult, in general, to obtain minimum porosity. If isometric solid spheres are packed in such a way that one sphere is surrounded by 12 spheres, the minimum porosity of packed spheres is computed theoretically as 26%. This situation is called as the "hexagonal closed packing". Many experiments on the mechanical packing of the isometric metal spheres showed that experimentally obtainable minimum porosity ranged between 36~44%. Most of the metallic spheres do not adhere to each other at ordinary room temperatures, but it was almost impossible to obtain the theoretical minimum porosity. These experiments suggest that comparatively spacious voids or pore spaces may be always created within the aggregates of solid particles. Solid particles hang and hold together and produce spacious pores within aggregates even if they do not entirely adhere to each other. This phenomenon is caused by the "arching" or "bridge making" of particles which arise from their surface irregularities and mutual friction. As described in the previous section, the natural snow crystals or pulverized snow particles posses not only large surface irregularities, but also they have proper cohesion. Therefore, their packing process may be strongly influenced by the surface irregularities and mutual cohesion. This suggests the possibility to draw some information on micromeritical properties of snow from their compaction process. This section will deal the compaction process of snow by tapping.

When a cylindrical container filled with snow is dropped repeatedly from a certain height h, the volume of snow V may be decreased as a function of numbers of tapping N, and then it will approach to the final values V_∞, the unchangeable volume by infinite application of the tapping. On the contrary, apparent density ρ of snow increases and approaches to the final density ρ_∞ obtained by the infinite tapping application. These situation are illustrated schematically in Fig. 12. In this figure, V_0, ρ_0 and V_∞, ρ_∞ represent the initial and the final volumes and densities of snow, and curves (1) and (2) show the compaction processes of the two different types of snow.

In order to characterize the micromeritical feature of snow found in the compaction

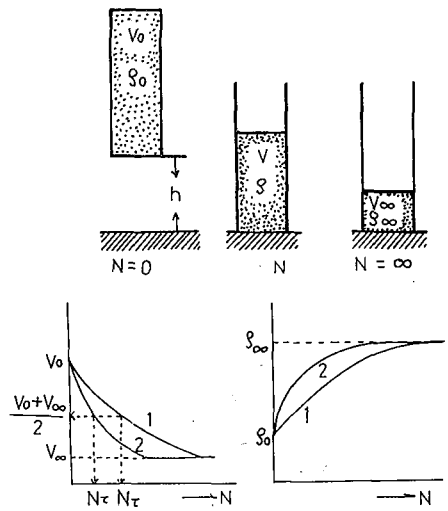

Fig. 12. Schematic diagrams of compaction process of snow by tapping

process, we shall define a dimensionless number $r=(V_0-V)/V_0$. r is called the "compaction ratio" or the "volume strain". The correlation between r and N was given empirically by Kawakita (1964) as follows:

$$r = \frac{abN}{1+bN}, \tag{1}$$

where a and b are numerical constants. In this equation, if we put $N=\infty$, r becomes a. Therefore, the physical meaning of a is the final compaction ratio or volume strain, r_∞, which should be obtained at the infinite tapping application. We have

$$a = \frac{V_0-V}{V_0} = r_\infty . \tag{2}$$

If we substitute the eq. (2) for a in eq. (1), we obtain

$$b = \frac{V_0-V}{N(V-V_\infty)} . \tag{3}$$

In eq. (3), if we put $V_0-V=V-V_\infty$, b comes

$$b = \frac{1}{N_\tau} , \tag{4}$$

where N_τ is the number of tappings required to decrease the initial volume of sample to the volume

$$V = \frac{1}{2}(V_0+V_\infty) .$$

If the initial volume of snow is decreased to $1/2\,(V_0+V_\infty)$ by only one application of the tapping, the value of b comes to 1. b is called the "velocity factor of the compaction".

Equation (1) can be rewritten as follows:

$$\frac{N}{r}=\frac{1}{ab}+\frac{1}{a}N. \tag{5}$$

If we plot observed values of N/r against N, the correlation between N/r and N may be expressed by a straight line. The value a and b can be computed from the slope and the intersection with the axis of N/r of this straight line.

The eq. (5), however, is not the only expression for the compaction process of snow. The following formula can be used to express density change of snow by tapping.

$$(\rho_\infty-\rho_n)=(\rho_\infty-\rho_0)\exp(-kN), \tag{6}$$

where, ρ_n is the apparent density obtained after N applications of tapping, and k is the numerical constant proportional to the velocity of the compaction. k is called the decay factor of the volume of snow.

2) *Experimental apparatus*

Figure 13 shows a schematic diagram of the experimental apparatus for the compaction of snow by tapping. In this figure, a is a cylindrical container made of brass. Its diameter and length are 3.6 and 20 cm respectively. After the cylinder was filled with snow, it was placed in the guide cylinder G. A small stick b was attached to the bottom of the cylindrical container a, and the end of this stick was in contact with the smooth surface of the cam driven by an electric motor. A step, 4 cm in depth, was cut in the periphery of the cam as shown by h. When the cam was rotated slowly in the direction shown by an arrow, the container was lifted up gradually and it was dropped abruptly at step h. As the rotating speed of the cam was 30 r.p.m., the container could be tapped every two seconds. The shrinkage of the volume of snow was measured through a transparent window slit made in the container.

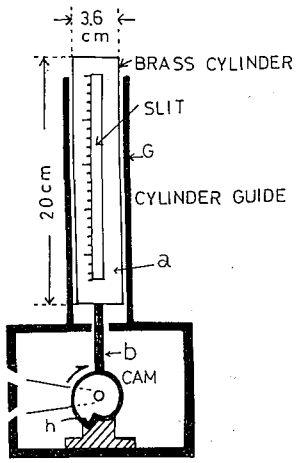

Fig. 13. Experimental apparatus for tapping of snow

3) *Experimental results*

a) Compaction of the dendritic snow crystals

Figure 14 illustrates a typical compaction process of the dendritic snow crystals. Snow crystals were stuffed in the container with the different initial densities such as ρ_0=0.032, 0.0437, 0.0759 and 0.138. As seen in this figure, the compaction ratio r of these four samples increased exponentially with the number of tapping as shown by curves I for ρ_0=0.032, II for ρ_0=0.0437, III for ρ_0=0.0759 and IV for ρ_0=0.138. Figure 15 shows the correlation between N/r and N for each sample. A linear correlation is seen between N/r and N. The numerical values of a and b computed from the slope and the intersection of these straight lines are listed in Table 2.

In this table, the values of initial densities ρ_0 and those of the final densities calculated from the values of the final compaction ratio a are listed. As seen in this table, a values were kept nearly constant in the range of the initial density 0.032~0.138, and the average value was found to be 0.6. This means that approximately 60% of the

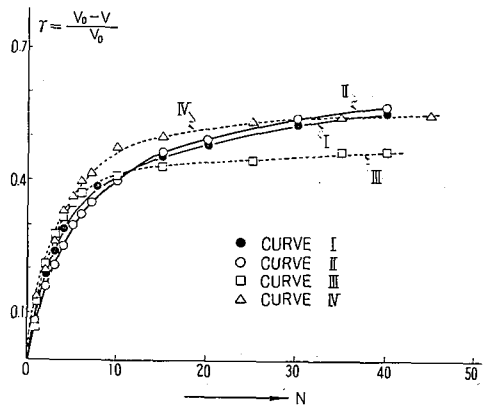

Fig. 14. Correlation between compaction ratio and number of tappings

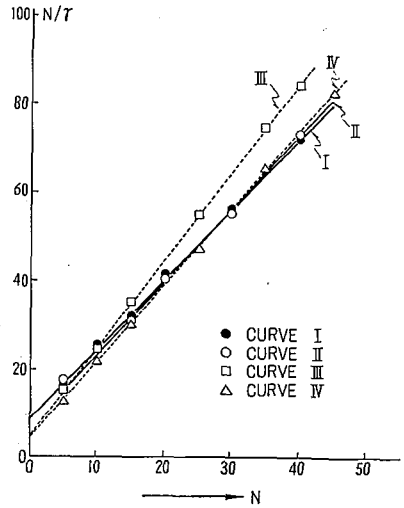

Fig. 15. Correlation between N/γ and N for dendritic snow crystals

Table 2. Final compaction ratio and velocity factor of compaction of snow crystals

Sample number	Initial density ρ_0	Final density ρ_∞	Final compaction ratio a	Velocity factor b
I	0.032	0.0885	0.638	0.189
II	0.0437	0.12	0.637	0.196
III	0.0759	0.16	0.52	0.427
IV	0.138	0.336	0.59	0.376

initial volume of snow may be compacted by infinite times of the tapping application. The velocity factor b showed a tendency to increse with the initial density of snow. As this value is closely correlated to the mechanism of the compaction process, we will discuss this problem in the following section.

b) Compaction velocity of snow

It appears that the compaction of snow proceeds as a simple exponential function of the number of the tapping as shown schematically in Fig. 12, but the actual mechanism of the compaction of snow is not always simple. If we plot logarithmically the density change $(\rho_\infty - \rho_n)$ of the dendritic snow against N, it may be seen that all curves have a critical point where the slope of the curve changes abruptly at a certain number of tapping as shown in Fig. 16. This situation means that the compaction process of snow can not be expressed by a simple exponential function of N, but it may be expressed approximately by the following two exponents

$$\rho_\infty - \rho_n \sim C_1 \exp(-k_1 N) + C_2 \exp(-k_2 N), \tag{7}$$

where C_1 and C_2 are constants and k_1 and k_2 are different decay constants, respectively. The numerical values of k_1 and k_2 computed from the slopes of these curves are listed in Table 3.

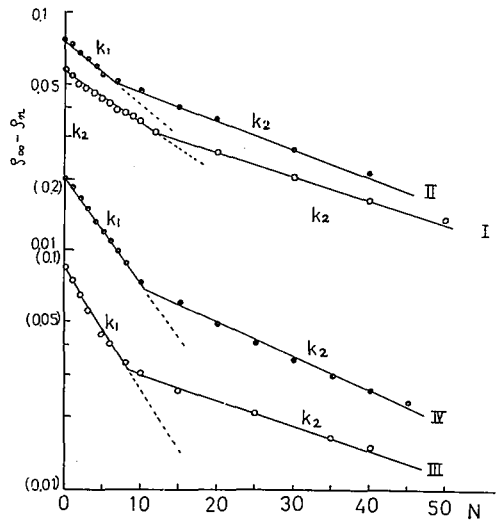

Fig. 16. Density change against tapping number N

Table 3. Velocity factors of compaction of dendritic snow crystals

Sample number	ρ_0	k_1	k_2	b
I	0.032	0.0515	0.0232	0.189
II	0.0437	0.0575	0.027	0.196
III	0.0759	0.115	0.0242	0.427
IV	0.138	0.0885	0.0329	0.376

In this table, b values are the velocity factor of compaction defined by eq. (4). As k_1, k_2 and b are the factors obtained for the same sample of snow, there must be a certain correlation between them. In order to examine this point, k_1 and k_2 were plotted against b as shown in Fig. 17. As seen in this figure, the correlation between k_1 and b (black circles) is represented by a straight line, but no linear relationship is found between k_2 and b as shown by the open circles. This means that b is related to only k_1. As shown in Fig. 16, the numerical values of k_1 were found to be larger than those of k_2, suggesting that the mechanism of compaction of snow may be changed with the number of tapping. In the initial stage of the tapping, the compaction may be made mainly by collapses of comparatively large pore spaces formed by arching or bridge making, but in the later stage of the tapping application, it may be achieved by overcoming the internal friction between crystals which arise from the surface irregularities and the proper cohesion.

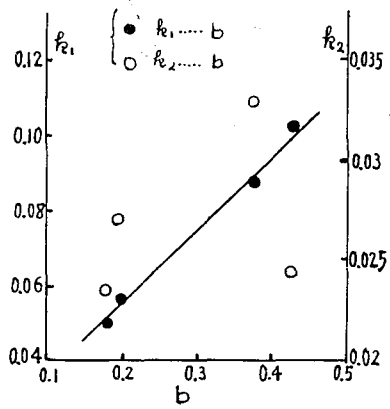

Fig. 17. Correlation between k_1, k_2 and b

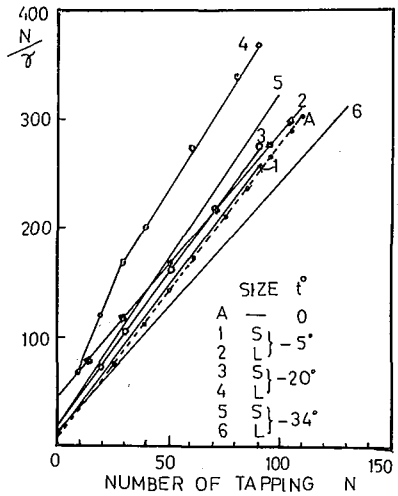

Fig. 18. Correlation between N/γ and N for pulverized snow particles

c) Compaction of pulverized snow particles

Two blocks of snow were pulverized into powder by rubbing against each other. The powdered snow was sieved into two classes, L and S. L means large particles passed the opening 2 mm of sieve and were retained by the opening of 0.84 mm, and S means small size particles less than 0.84 mm in diameter. In order to examine the temperature and size dependence of the compaction factor of these two kinds of snow, the tapping was conducted at various temperatures at 0, −5, −20 and −35°C. Figure 18 shows correlations between N/γ and N for these samples. Curves numbered from 1 to 6 are dry snow, and number A is wet snow. In the case of wet snow, the experiment was conducted at room temperature of +2°C. Four experiments were made for wet snow, but no difference was observed.

Various experimental data obtained for the compaction of the pulverized snow are listed in Table 4. As seen in Table 4, the final compaction ratio a of the pulverized snow did not change with grain size, temperature,

Table 4. Final compaction ratio and velocity factor of compaction of pulverized snow

Sample Nos.	Temp. °C	Grain size	Density ρ_0	Density ρ_∞	Porosity p_0	Porosity p_∞	Final compaction ratio a	Velocity factor for compaction b	k_1	k_2	Remarks
1	− 5	S	0.223	0.344	0.757	0.628	0.37	0.24	0.085	0.026	
2	− 5	L	0.155	0.25	0.832	0.728	0.38	0.24	0.085	0.015	
3	−20	S	0.186	0.27	0.798	0.706	0.35	0.18	0.075	0.04	Dry
4	−20	L	0.165	0.22	0.821	0.760	0.33	0.045	0.087	0.025	snow
5	−34	S	0.140	0.25	0.848	0.728	0.33	0.25	0.07	0.019	
6	−34	L	0.114	0.21	0.876	0.771	0.42	0.11	0.034	0.019	
A	0		0.292	0.485	0.683	0.466	0.35	0.45	0.23	0.013	
A	0		0.315	0.56	0.658	0.390	0.35	0.45	0.1	0.0137	Wet
A	0		0.362	0.601	0.606	0.348	0.35	0.45	0.1	0.0317	snow
A	0		0.316	0.53	0.658	0.425	0.35	0.45	0.09	0.015	

and its state, dry or wet, the average value of it was nearly 0.36. This value is very small as compared with that of dendritic snow crystals. The difference of a between dendritic snow crystals and pulverized snow (0.6∼0.36) may arise from the difference in their geometrical shapes. Dendritic snow crystals are so thin and two dimensional that they may be compacted readily, but pulverized snow particles may not be densely compacted, because they are spherical and three dimensional. As seen in Table 4, some interesting tendencies can be seen in the velocity factor b, *eg.* comparatively small grains

marked by S posses larger values of b than those of large grains marked by L. This tendency implies that small grains cause easy arching or bridge making as compared with large grains. When ice particles were wetted, large spacious pores were introduced within aggregates because of liquid water film and gave rise to larger values of b than those of dry snow.

IV. Age Hardening and Capillary Potential of Pulverized Snow

1) *Age hardening of pulverized snow*

Ordinary powders, metallic or non-metallic, do not cake or consolidate at room temperatures, but they begin to coagulate when the temperature is elevated to a point below the melting point. Ordinary climatical low temperatures are very close to the melting point of ice. The consolidation process of snow is very similar to the sintering process analogus to the powder metallurgy or ceramics. When ice particles are brought into contact, ice bonds begin to grow at the contact points. The ice bonding or neck growth is created by the transportation of water molecules from other portions of particles to the contact points. The driving force to cause this transportation may arise from the difference of the chemical potential between the neck and other parts of the particles. The sintering process of ice has been investigated by Kingery (1960) and Kuroiwa (1961), but its mechanism is still in dispute. Apart from the mechanism of the sintering, it may be true that the consolidation of snow is accompanied by the reduction of the surface area and the decrease of air voids or pore spaces within the snow. Thus, sintering of natural snow may proceed as a function of the temperature and the lapse of time, and give rise to age hardening.

In order to examine the correlation between age hardening and ice bonding of snow particles, the following experimentations were conducted. The pulverized snow particles were stuffed homogeneously in a wooden frame, $35\times15\times4$ cm, with an apparent density of 0.51. After several hours, the frame was carefully removed, leaving a square snow aggregate. This snow aggregate was cut into several rectangular bars, $30\times4\times1.5$ cm in dimension. A pair of the rectangular bars were covered with polyethylen sheets and placed in the three different cold rooms maintained at -3, -12 and -35°C to sinter them for a long time. In order to investigate and compare the age hardening of these snow aggregates in which the sinterings are proceeding at different temperatures, the measurements of Young's modulus of the specimens were made in the cold room kept at -20°C. When the specimen was transfered from the individual cold room, approximately 30 minutes were necessary until the temperature of the specimen coincided with -20°C. Young's modulus was measured by the flexual vibration method developed by one of the authors (1965). Immediately after the measurement, the specimen was returned again to the original cold room to continue sintering. Simultaneously with the measurements of Young's modulus, a small part of another rectangular bar stored in the same cold room was cut to make a thin section by the aniline method (Kinosita and Wakahama, 1960). After taking microphotographs of the thin section, the width of ice bonds grown at the contact points of snow particles was measured statistically. Both measurements, Young's modulus and ice bond growth, were conducted intermittently during the sintering periods.

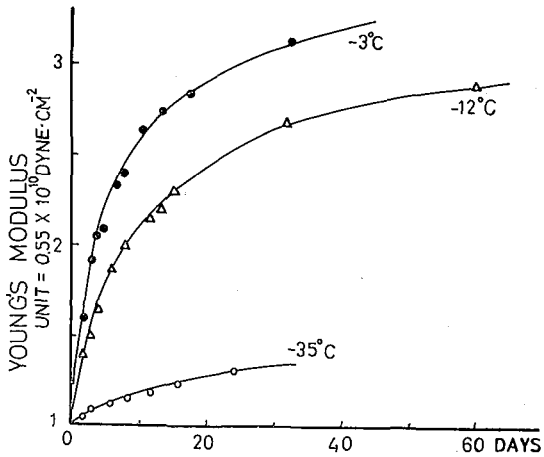

Fig. 19. Change of Young's modulus with sintering time and temperatures

Figure 19 shows the changes of Young's modulus of these three kinds of specimens sintered at different temperatures. The abscissa is the sintering time. The ordinate is the magnitude of Young's modulus expressed by the unit of 0.55×10^{10} dyne/cm^2. This unit was the initial value of Young's modulus measured immediately after the stuffing. As seen in this figure, Young's modulus increased exponentially with the time, showing a large rate of increment with the sintering temperatures. The width of ice bonds or neck growth developed between grains was measured on the enlarged microphotographs of the thin sections, and they were classified into groups every 20 μ to depict a frequency distribution curve. The change of frequency distribution curves of the width of neck growth observed at -3°C is illustrated as a function of the sintering time in Fig. 20. Immediately after the stuffing of pulverized snow, the mode of ice bond distribution was

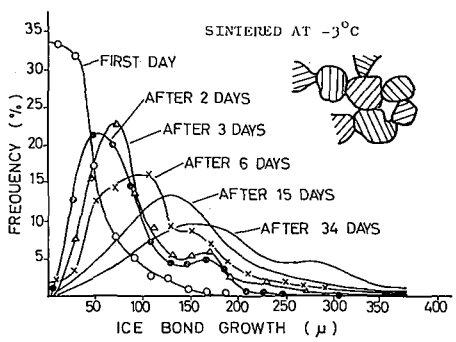

Fig. 20. Change of frequency distribution curves for ice bond growth

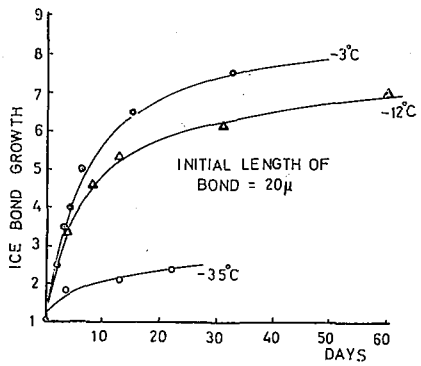

Fig. 21. Ice bond growth as a function of time and of temperature

20 μ as shown by the curve of the first day, but it shifted towards a larger size with the lapse of time. The average value at which the maximum of frequency appears was plotted as shown by curve of -3°C in Fig. 21. Similar data obtained at -12 and -35°C are plotted in Fig. 21. The ordinate is the magnitude of ice bond growth

expressed by the unit of initial size $= 20\,\mu$. As seen in this figure, the ice bonds developed with time and sintering temperature in the same manner as Young's modulus. This similarity suggested a close correlation between the age hardening and neck growth within the aggregate.

2) *Capillary potential of snow*

Consolidation or sintering of powered materials proceeds by the reduction of the surface areas of particles and the decrease of the voids or pore spaces. When two particles are brought into contact, the apparent surface energy of this joined system may be increased over that of the equiliburium form of the system. The main force to cause the sintering is considered to be the excess surface energy which arises from the surface irregularities and contacts between particles.

In this section, we shall define a capillary potential of the pulverized snow and investigate it from the point view of the sintering. The pulverized and sieved snow particles were stuffed in a glass cylinder, and tapped by dropping from a height of 3~4 cm, until the homogeneous packing of snow could be attained. When the end of this cylinder was soaked vertically in kerosene, the kerosene began to penetrate up within the snow by the capillary action. The capillary potential of snow can be defined by ρgH, where ρ is the density of kerosene, g the gravity acceleration, H the equilibrium height or the head of the penetrated kerosene measured from the original level. Both ρ and g are constant, hence H can be used as an expression of the capillary potential of snow.

In order to demonstrate how the capillary potential of snow varies with the consolidation or sintering process, the following experimentations were conducted in the cold room maintained at -5°C. In these experiments, five glass cylinders, 3.2 cm in diameter and 20 cm in length, were prepared, and the same mass of the pulverized snow was stuffed in these cylinders by tapping in such a way that the apparent density of snow in the cylinders became approximately the same as 0.58. Immediately after the stuffing, one of the cylinders was stood vertically in a wide and shallow pan filled with kerosene maintained at -5°C (see Fig. 22). The level of the kerosene was kept constant during the experiment. The head of the penetrated kerosene was measured with the time from the moment of the immersion until equilibrium was attained. The other four cylinders were stored in the cold room for diffrent periods of sintering. After a certain time elapsed, these cylinders were soaked in a kerosene pan to measure the individual capillary potential.

Figure 22 shows variations of the kerosene head with time for these five samples. In this figure, curve (a) illustrates the change of H of the sample measured immediately after the stuffing. As seen in this curve, the kerosene began to penetrate very rapidly into the snow from the moment at which the end of the cylinder was soaked in the kerosene. Then the head of kerosene attained a quasi-equilibrium after 1 hour or so. Curve (b), (c), (d) and (e) show changes of the kerosene heads of the samples sintered for 2, 5, 20 and 44 hours. As seen in these curves, the capillary potential H was increased with the increase of sintering periods. This result strongly suggests that the capillary potential of snow can be enhanced by the sintering.

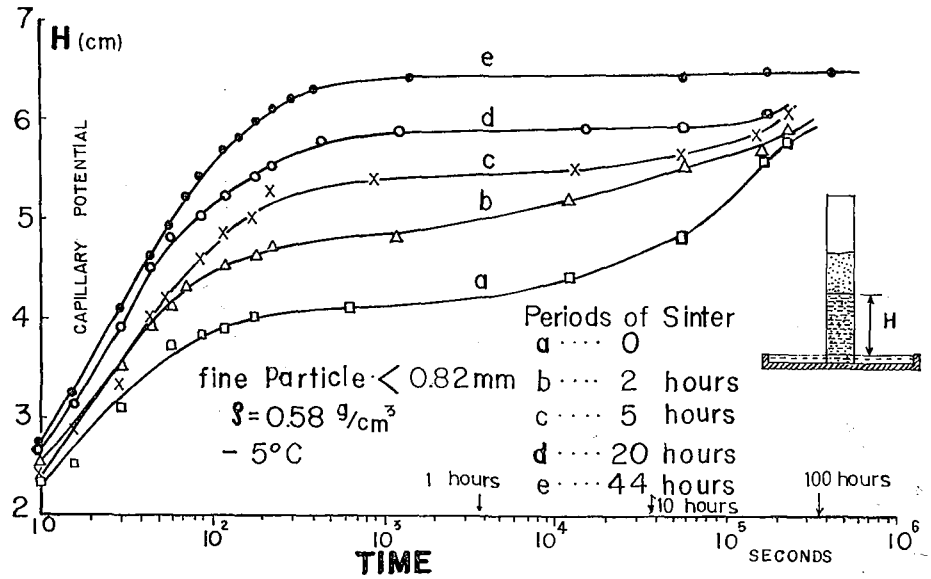

Fig. 22. Change of capillary potential of pulverized snow as the function of sintering period

The penetration of the kerosene may be created by the depression of the internal pressure within the snow aggregate, and the depression of the internal pressure may be caused by the capillarity given by $2\delta/r$, where δ is the interfacial energy between ice and kerosene, r is the effective radius of the curvature of the pores. In this argument, it is assumed implicitly that the pore spaces in snow aggregate are composed of the isometric imaginary capillary tubes. According to our experiments, the capillary potential of the snow which had been sintered for a long time was higher than that of snow sintered for short period, and no change was observed in the apparent density of the sample before and after the sintering. This means that the radius of curvature of the imaginary capillary tubes in the snow aggregate became smaller and smaller with the increase of sintering time, provided that the apparent density was kept constant. As seen in curve (a), the kerosene began to rise again in the snow after the quasi-equilibrium was attained, and approached gradually to the curve (e). A similar tendency can be seen in the curves (b) and (c). This phenomenon may be understood if we recognize that the sintering proceeded in the remaining portion of the snow which had been unwetted by the kerosene.

Similar experimentation was conducted at $-15°C$, but no appreciable change of the capillary potential was observed except for a little change in the velocity of the penetration of the kerosene.

V. Concluding Remarks

Natural snow crystals and pulverized snow were studied from the point of view of micromeritics or physics of powder. The most basic micromeritical properties of snow

are the surface roughness or irregularity and the proper cohesion of ice particles. A simple definition on surface irregularity was given for natural snow crystals and pulverized snow particles, and numerical values of the irregularity were measured according to the definition. The observed values of irregularities ranged within 40~20 for dendrites, 7~5 for sector and needle like crystals, and 3~1 for pulverized snow. The angle of repose, one of the important properties of powders, is strongly influenced by the surface properties of snow crystals or ice particles. The following experimental results were obtained. The values of angle of repose measured at −35°C were approximately 45 deg for pulverized snow, 63 deg for natural snow crystals composed of dendrites. As the influence of cohesive force on the angle of repose were so small at −35°C, this difference may be attributed to the difference of the surface irregularities between snow crystals and pulverized snow. The angle of repose of the pulverized snow approached to 90 deg when the temperature was elevated to a point near the melting point. In the case of the dendritic snow crystals, it could be regarded as 90 deg in temperatures above −12~−10°C. When snow crystals or pulverized snow are packed in a container by tapping application, the compaction process may be influenced by the surface irregularities and mutual adhesion of particles. The final compaction ratio a and the velocity factor of compaction b were measured. The obtained numerical values of a were 0.6 for dendritic snow crystals, 0.35~0.4 for pulverized snow particles. This result implies that the dendritic snow crystals can be more readily packed than the pulverized snow, because of their spacious configuration and easy arching properties. The pulverized snow particles may not be densely packed because of their three dimensional shapes. The velocity factor of the compaction b depends upon the spacious stractures in the aggregate. These spacious structures are created by the arching or bridge making and proper cohesion of particles. From the observation of the packing process, it was concluded that the volume of snow is compacted rapidly in the initical stage of the tapping application because of the collapsing of comparatively large spaces within the snow aggregate, then packing proceeds slowly by overcoming of internal friction between the snow particles.

Consolidation or coagulation is the most important properties of snow. This phenomenon is caused by sintering between particles. Age hardening of Young's modulus and capillary potential of snow aggregates were observed and discussed from the point of view of the sintering process.

References

1) HOSLER, C. L. JENSEN, CAPT. D. C. and GOLDSHLAK, Pvt. Leon 1957 On the aggregation of ice crystal to form snow. *J. Meteorol.*, **14**, 415-420.

2) KAWAKITA, K. 1964 Chemistry of powder. *Res. Rept. Hôsei Univ.*, **1**, 17-31. (In Japanese).

3) KINGERY, W. D. 1960 Regelation, surface diffusion and ice sintering. *J. Appl. Phys.*, **31**, 833-000.

4) KINOSITA, S. and WAKAHAMA, G. 1960 Thin sections of deposited snow made by the use of aniline. *Contr. Inst. Low Temp. Sci.*, **15**, 35-45.

5) KUROIWA, D. 1961 A study of ice sintering. *Tellus*, **13**, 252-259.

6) NAKAYA, U. 1954 Snow Crystals, Harvard Univ. Press, Cambridge, Mass., 510 pp.

7) NAKAYA, U. and MATSUMOTO, A. 1954 Simple experiment showing the existence of a "liquid-water" film on the ice surface. *J. Colloid. Sci.*, **2**, 41–49.